Applications of direct forcing immersed boundary method on calculation of loading in smoothed particle hydrodynamics method

Ming-Jyh Chern

Computational Fluid Dynamics Laboratory
Mechanical Engineering Department
National Taiwan University of Science and Technology

Motivation

Figure : Top: oyster wave energy converter (*source: subseaworldnews.com*). Bottom: Offshore pipeline jetty(*source: subseaworld.com*). The accurate prediction of hydrodynamic loading is important for ensuring the reliability and performance of an offshore structure.

SPH for FSI: The challenge

SPH is suitable for free surface flow simulation. However, there are some problems:

- The pressure field is plagued with noise.
  - δ-SPH and ISPH methods are developed to overcome this problem.
- If the conventional surface integration of the fluid stress is used,
  - a complex boundary condition algorithm is required to get accurate fluid stress and,
  - it could be difficult to obtain the normal vector for a complex geometry.

Objectives

- Apply DFIB method to model the immersed solid in combination with δ-SPH method for the accurate prediction of hydrodynamic loading.
  - DFIB simplifies the evaluation of hydrodynamic force using volume integral of the virtual force.
- Apply the method to study an oscillating cylinder beneath a free surface.

Governing equations

Continuity equation

$$\frac{\mathrm{D}\rho}{\mathrm{D}t} + \mathbf{u} \cdot \nabla\rho = 0$$

Momentum equation

$$\frac{\mathrm{D}\mathbf{u}}{\mathrm{D}t} = -\frac{\nabla p}{\rho} + \frac{1}{Re}\nabla^2\mathbf{u} + \mathbf{g} + \mathbf{f}$$

Equation of state

$$p = c_0^2(\rho - 1)$$

Direct forcing immersed boundary method

- A virtual force term is added into the momentum equation to enforce the non-slip boundary condition. The formula of the virtual force is denoted by

$$\mathbf{f}_i = \eta_i \frac{\mathbf{u}_s - \mathbf{u}_i}{\Delta t},$$

  where $\mathbf{u}_s$ is the prescribed solid velocity and η is the volume of solid (VOS) function.
- The hydrodynamic force can be calculated from the volume integral of the virtual force,

$$\mathbf{F} = -\iiint \mathbf{f} \mathrm{d}\forall$$

Direct forcing immersed boundary method

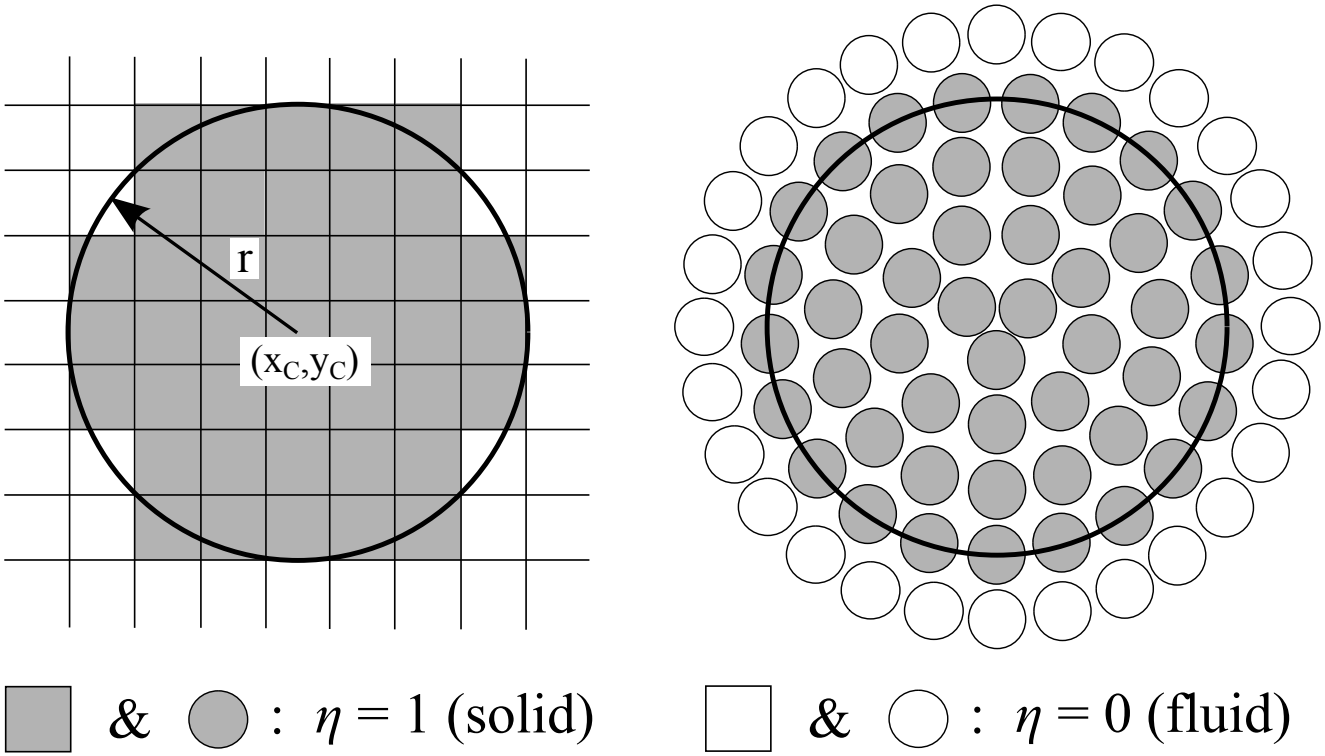

Figure : Volume of solid (VOS) function in grid-based and SPH methods. In the grid-based method, the VOS function can not represent the geometry exactly. This problem can be avoided in SPH by distributing some particles along the boundary of the solid object.

Continuity equation in δ-SPH form

$$\frac{\mathrm{D}\rho_i}{\mathrm{D}t} = -m_j \sum_j (\mathbf{u_j} - \mathbf{u_i}) \cdot \nabla_i W_{ij} + \delta h c_0 \sum_j \Psi_{ij} \cdot \nabla_i W_{ij} \forall_j$$

where $\delta = 0.1$ and

$$\Psi_{ij} = 2(\rho_j - \rho_i) \frac{\mathbf{r_{ji}}}{|\mathbf{r_{ij}}|^2} - \left[< \nabla\rho >_i^L + < \nabla\rho >_j^L \right]$$

Momentum equation in SPH form

$$\frac{\mathrm{D}\mathbf{u}_i}{\mathrm{D}t} = -\sum_j \left(\frac{p_j}{\rho_j^2} + \frac{p_i}{\rho_i^2}\right) \cdot \nabla_i W_{ij} m_j + \frac{1}{\mathrm{Re}} \left[\sum_j \frac{4\pi_{ij}}{(\rho_i + \rho_j)} \nabla_i W_{ij} m_j \right.$$
$$\left. - 2\sum_j (\mathbf{u_j} - \mathbf{u_i}) \nabla_i W_{ij} \frac{m_j}{\rho_j} \cdot \sum_j \nabla_i W_{ij} \frac{m_j}{\rho_j} \right] + \mathbf{g}_i + \mathbf{f}_i$$

where $\pi_{ij} = \dfrac{(\mathbf{u_j} - \mathbf{u_i}) \cdot \mathbf{r}_{ji}}{|\mathbf{r}_{ij}|^2}$

Quintic Wendland Smoothing Kernel

$$W = \alpha \begin{cases} (1-\frac{q}{2})^4(2q+1) & 0 \le q \le 2 \\ 0 & q > 2 \end{cases}$$

where $\alpha = \dfrac{7}{4\pi h^2}$ for a 2-D problem.

$$\frac{\partial W}{\partial q} = \frac{7}{4\pi h^3} \begin{cases} -5q(1-\frac{q}{2})^4 & 0 \le q \le 2 \\ 0 & q > 2 \end{cases}$$

Numerical procedure in a time step

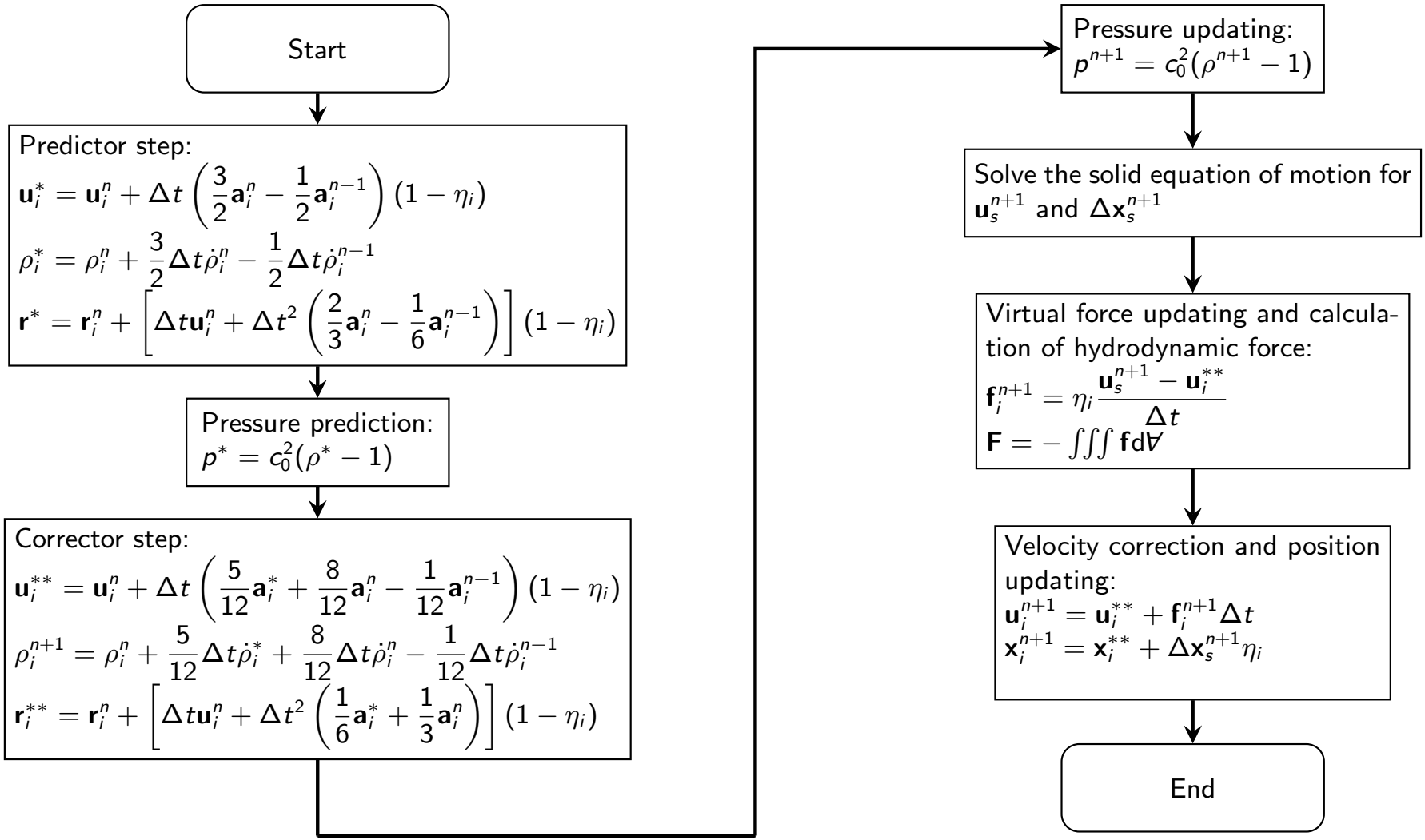

Lid-driven cavity flow over immersed cylinder

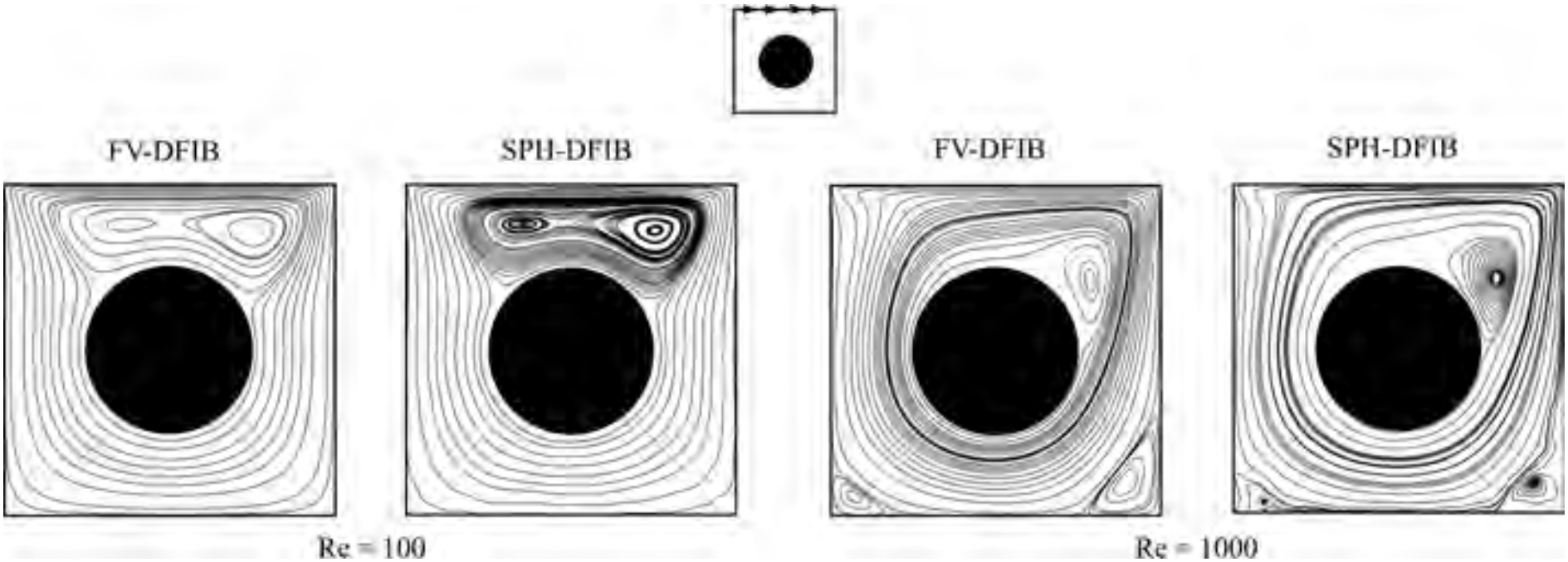

Figure : Streamlines at Re =100 and 1000.

Lid-driven cavity flow over immersed cylinder

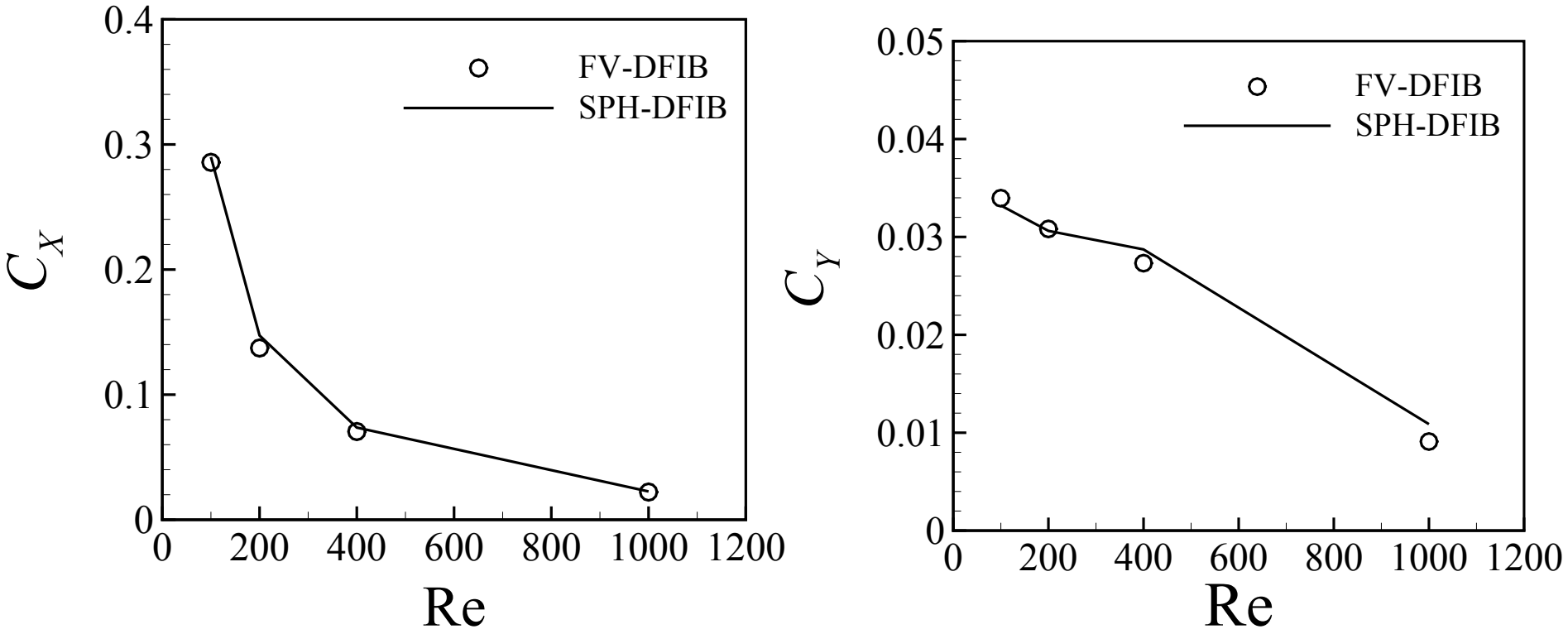

Figure : Comparison of transverse and in-line force coefficient.

Oscillating cylinder in a quiescent fluid at KC=3 and Re=100

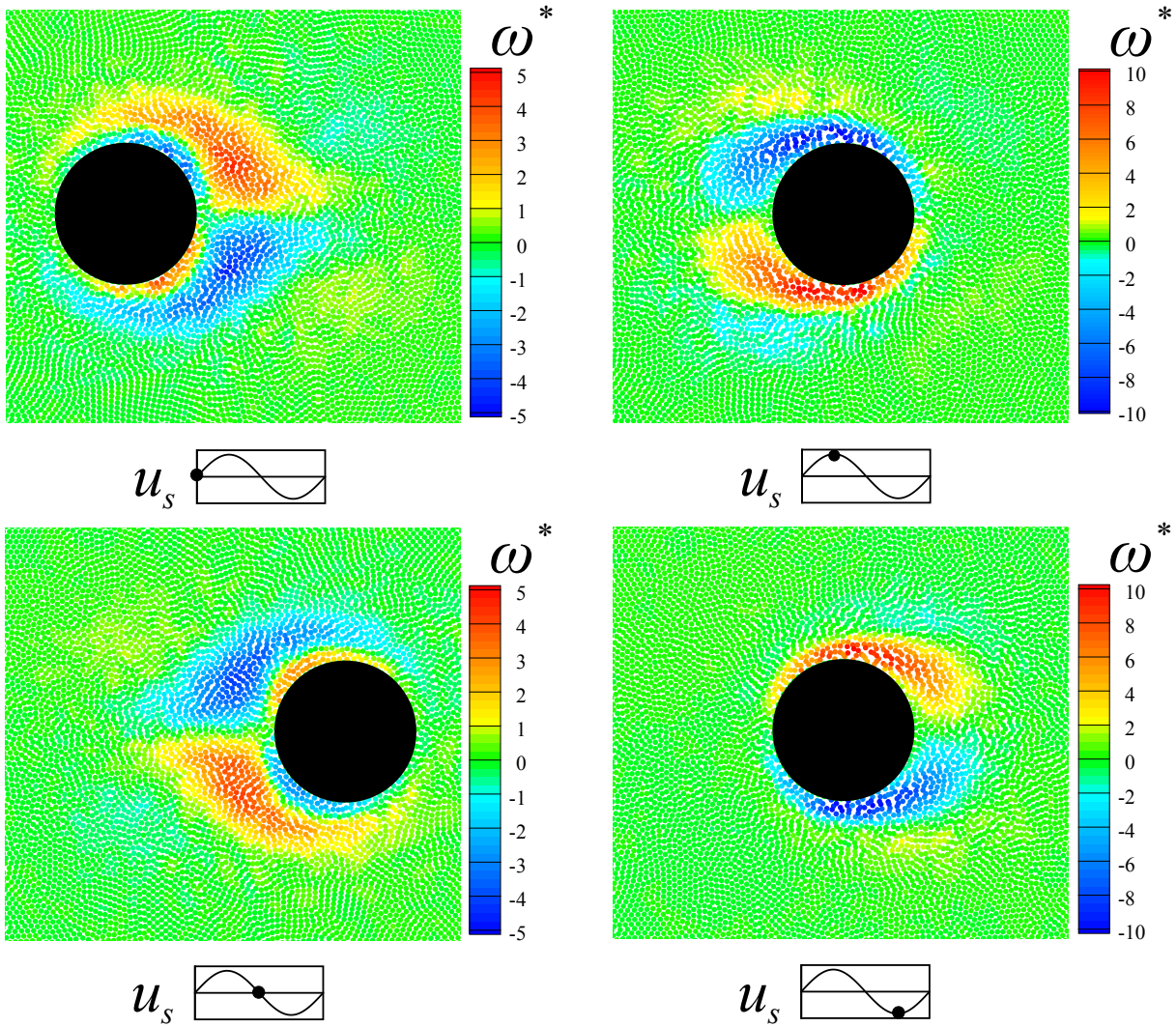

Figure : Instantaneous vorticities at various cylinder positions.

Oscillating cylinder in a quiescent fluid at KC=3 and Re=100

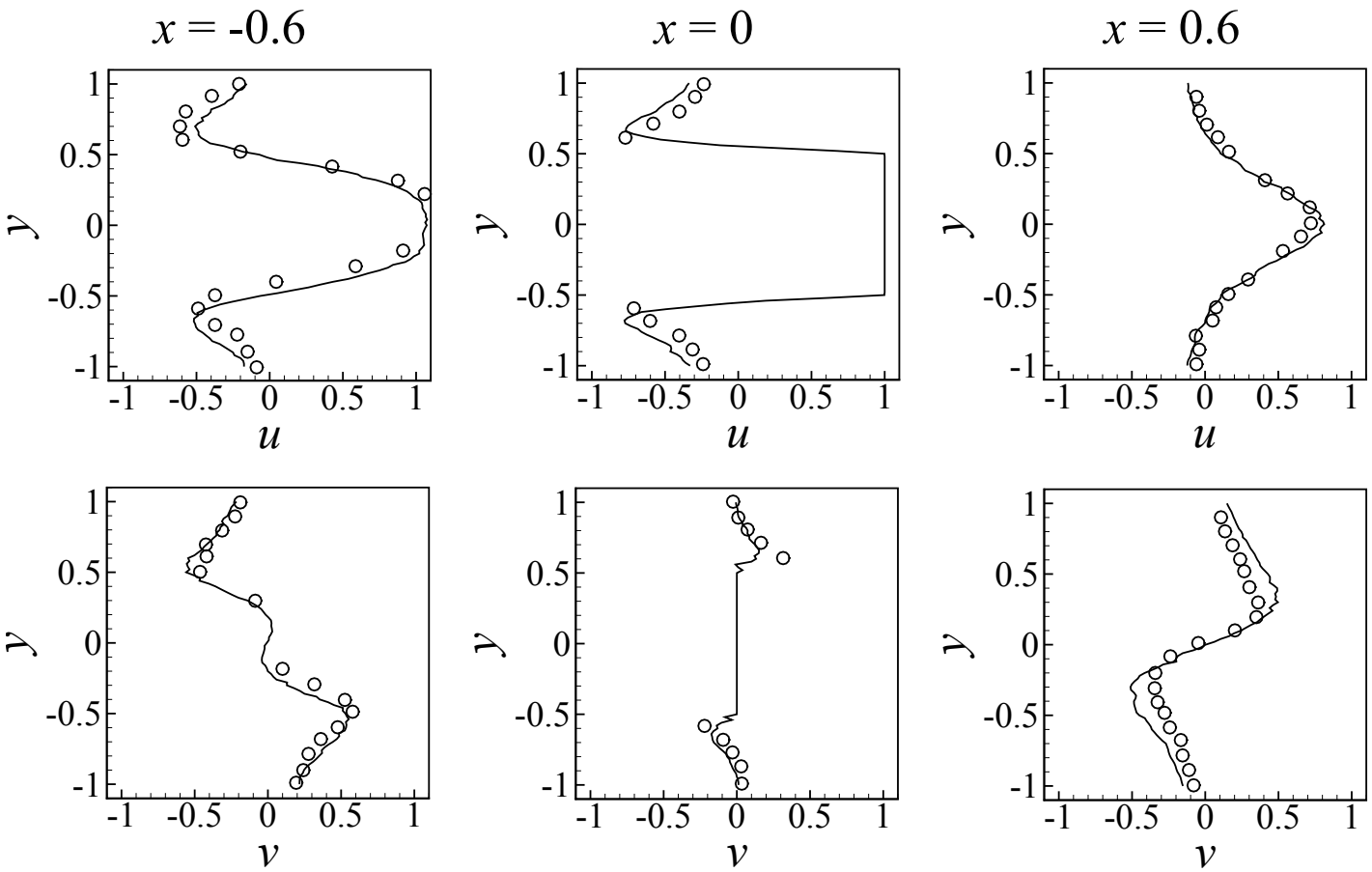

Figure : Comparison of velocity profiles when the phase angle of the cylinder is 180^o predicted by the present study (—) and Dutsch *et al.* (◯).

Dütsch, H., Durst, F., Becker, S., Lienhart, H., 1998. Low-Reynolds-number flow around an oscillating circular cylinder at low KeuleganCarpenter numbers. J. Fluid Mech. 360, 249271.

Oscillating cylinder in a quiescent fluid at KC=3 and Re=100

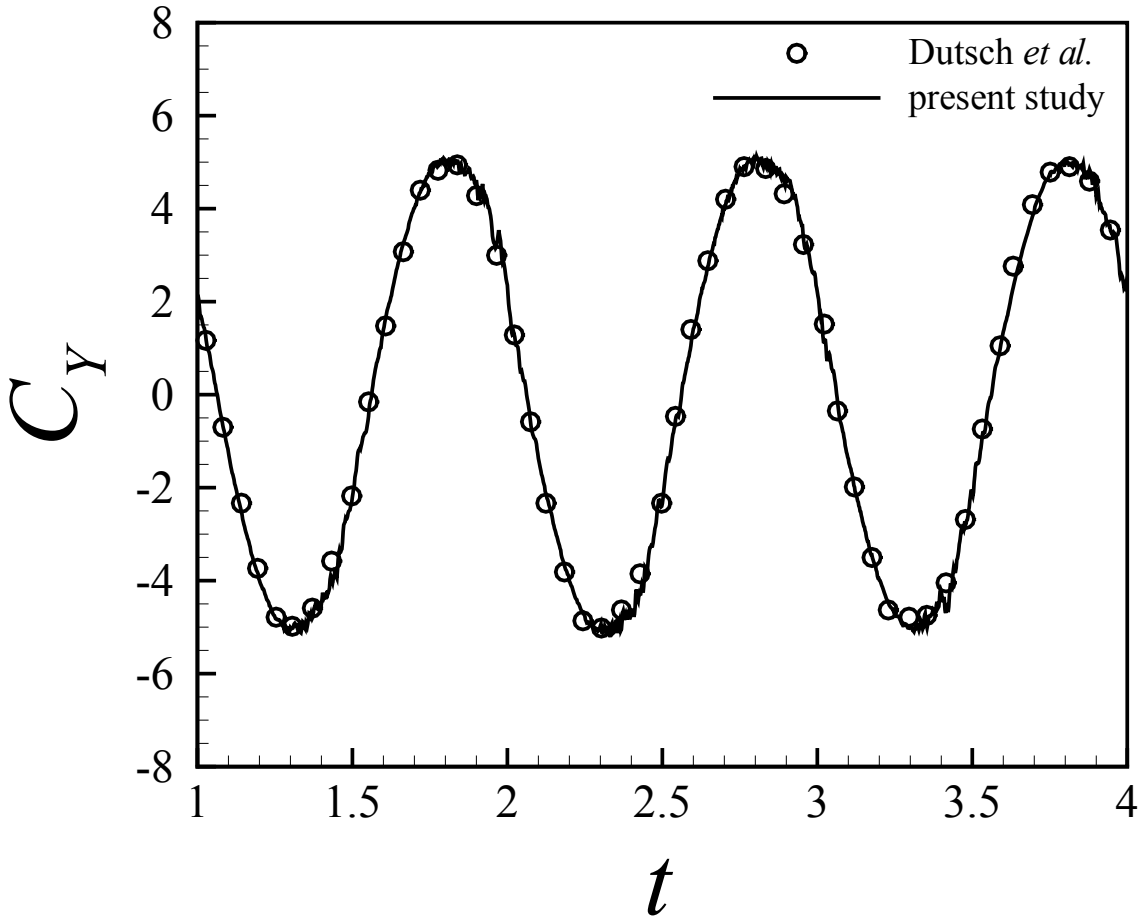

Figure :
Comparison of the time history of transverse force coefficient predicted by the present study (—) and Dutsch *et al.* (◯).

Dütsch, H., Durst, F., Becker, S., Lienhart, H., 1998. Low-Reynolds-number flow around an oscillating circular cylinder at low KeuleganCarpenter numbers. J. Fluid Mech. 360, 249271.

Oscillating cylinder close to a free surface

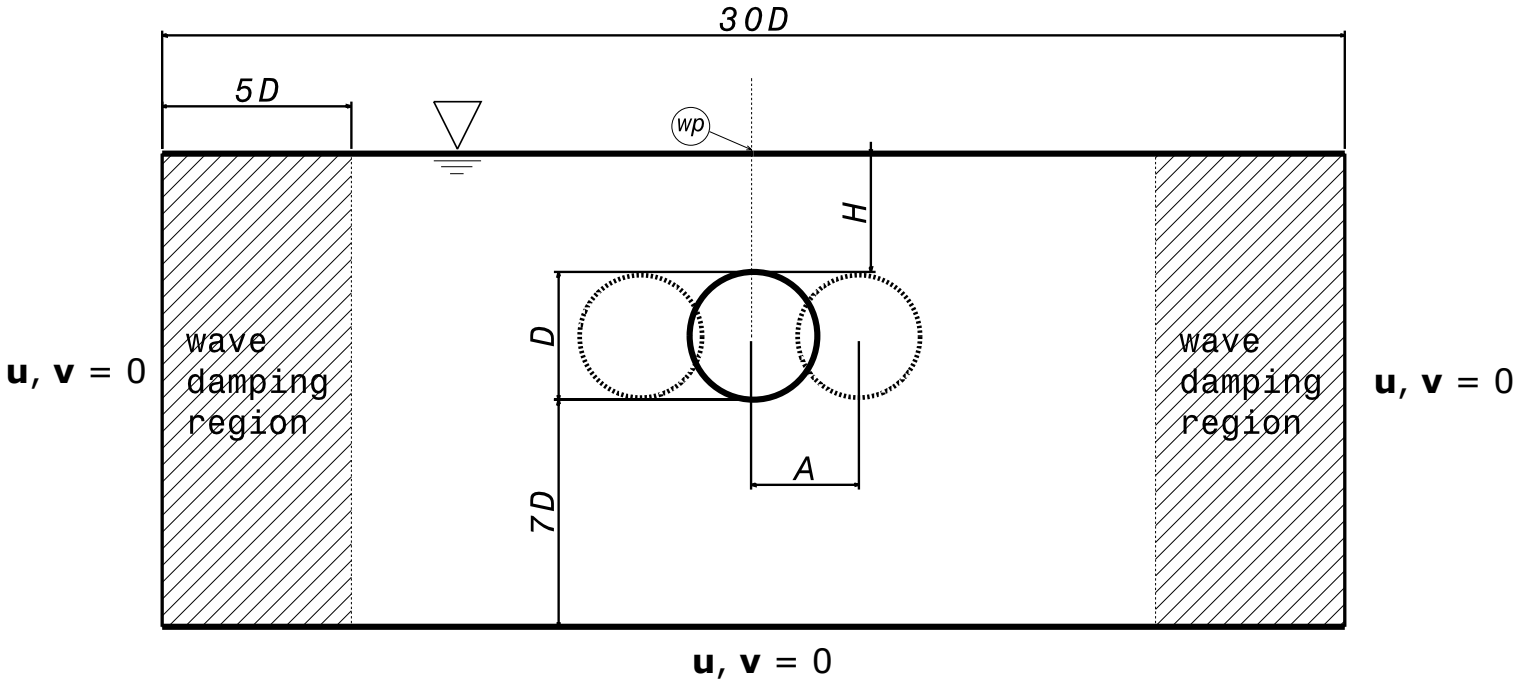

Figure : Schematic description of the case. Simulations are performed at Fr $= 0.35$, Re $= 100$, KC=3, 7, 10, and $H/D = 0.5 - 2.0$

Oscillating cylinder close to a free surface: Flow pattern map

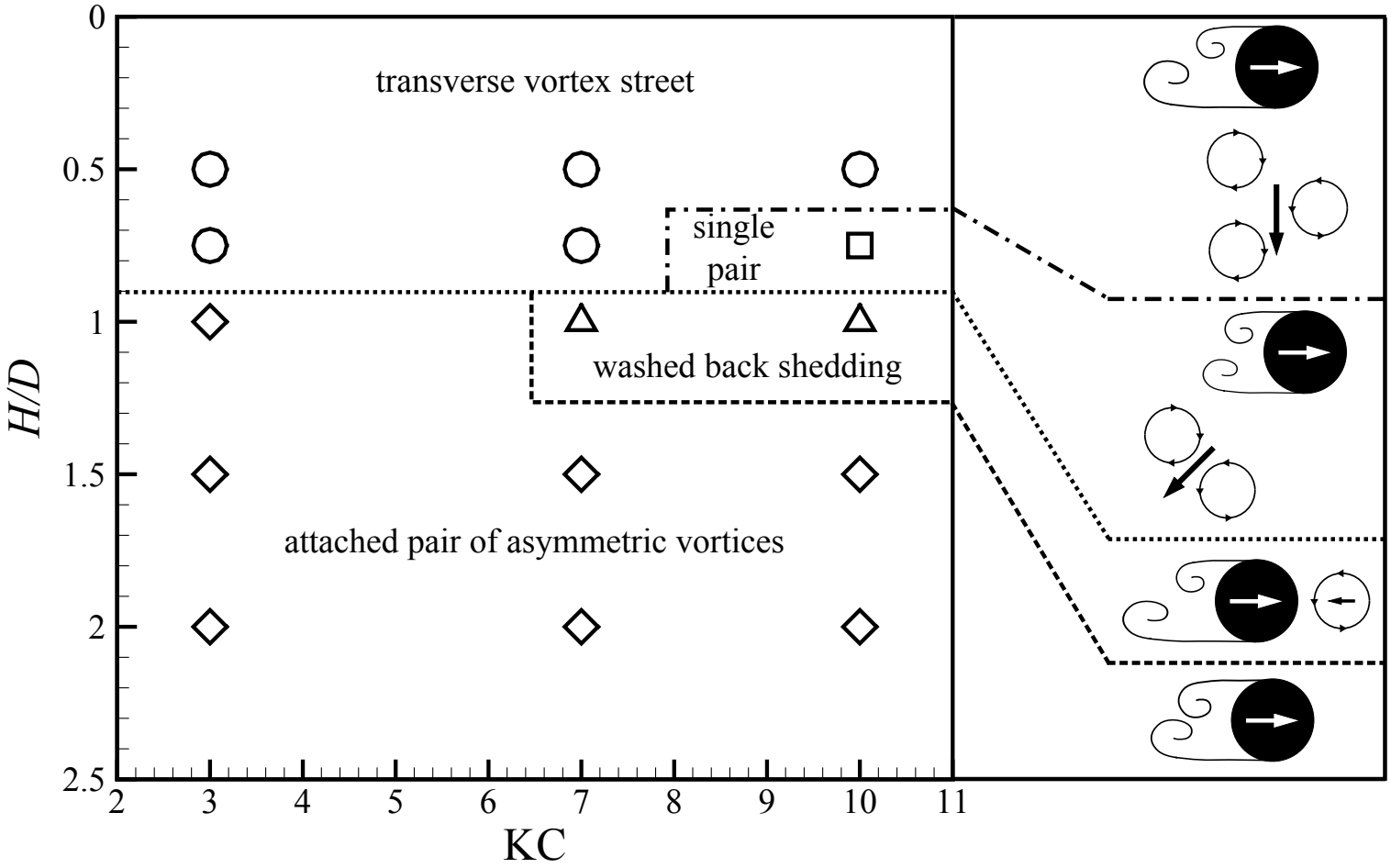

Attached pair of asymmetric vortices

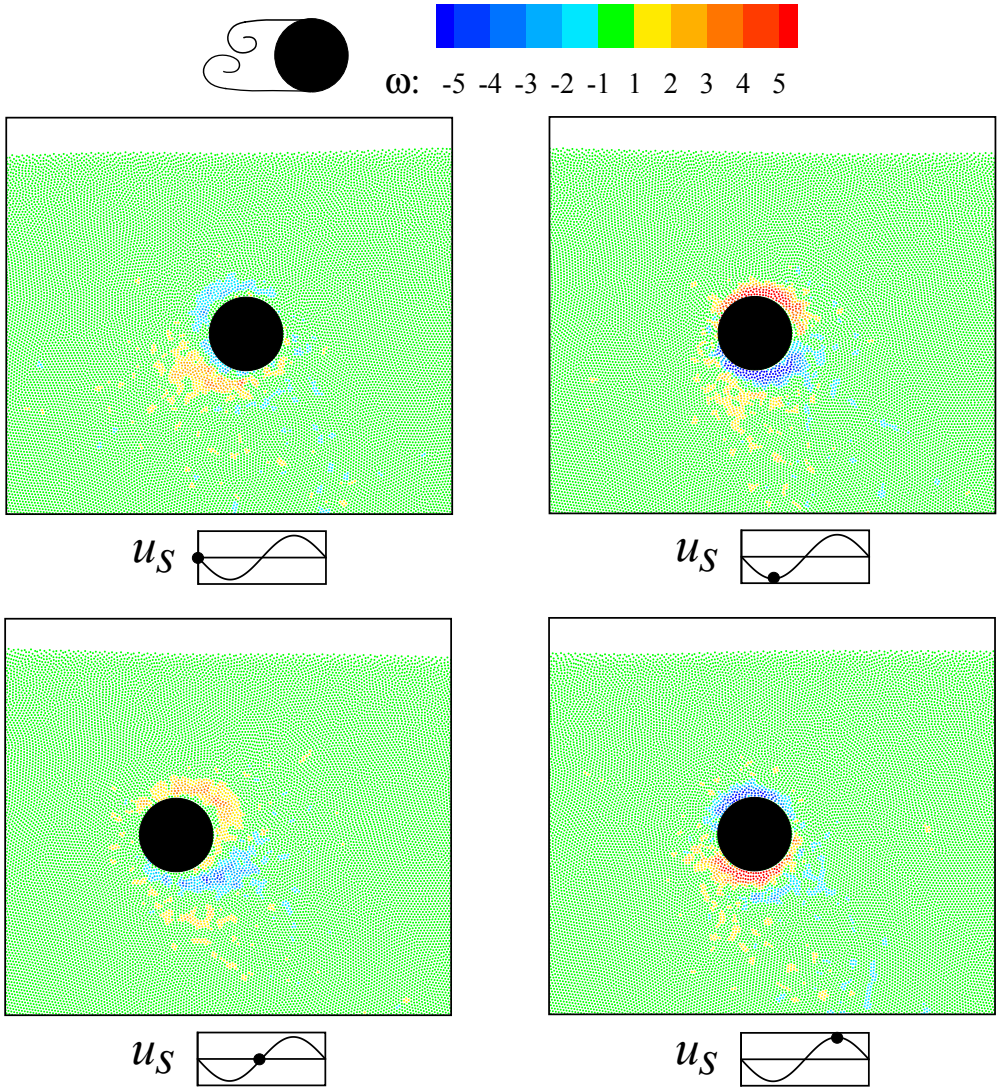

Figure : Vorticity contour at KC $= 3$ and $H/D = 2$.

Washed back shedding

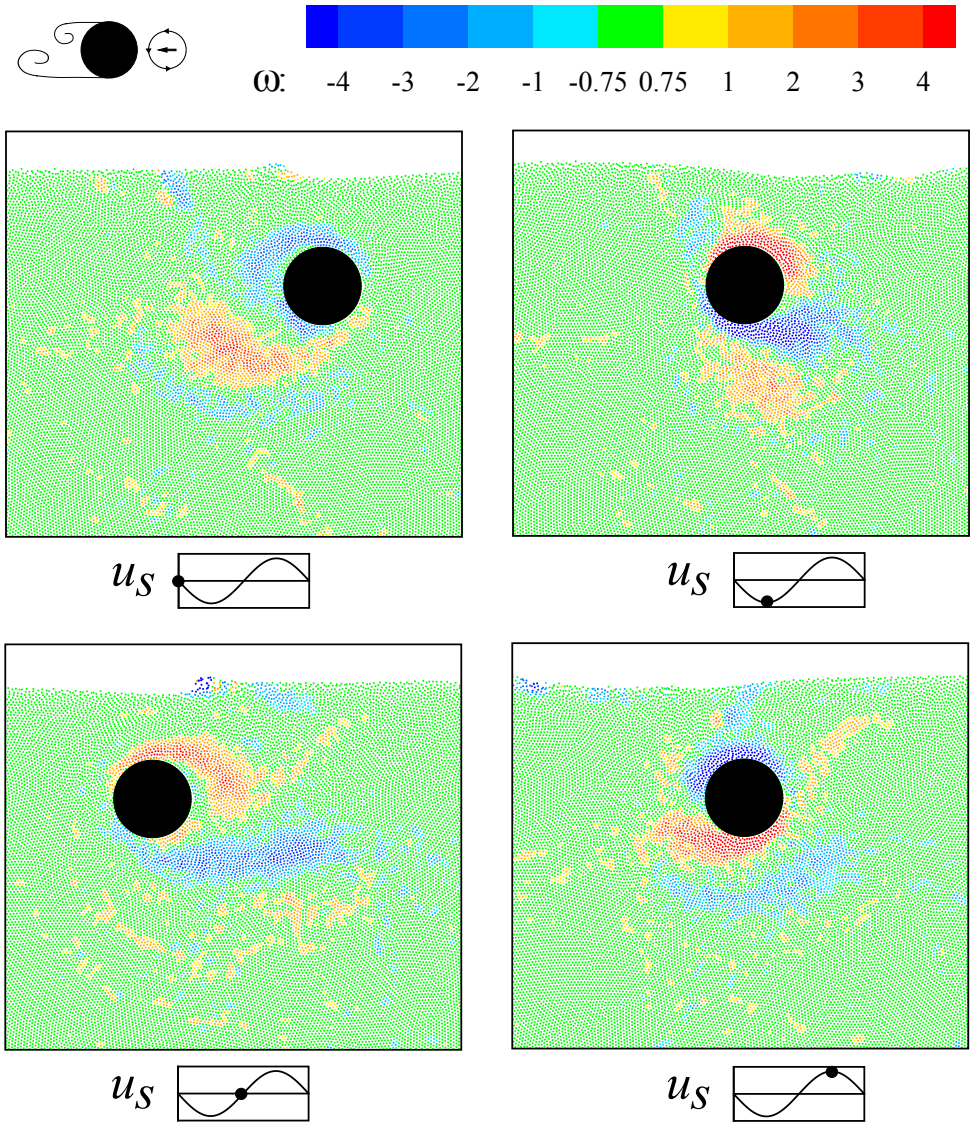

Figure : Vorticity contour at KC $= 7$ and $H/D = 1$.

Single vortex pair

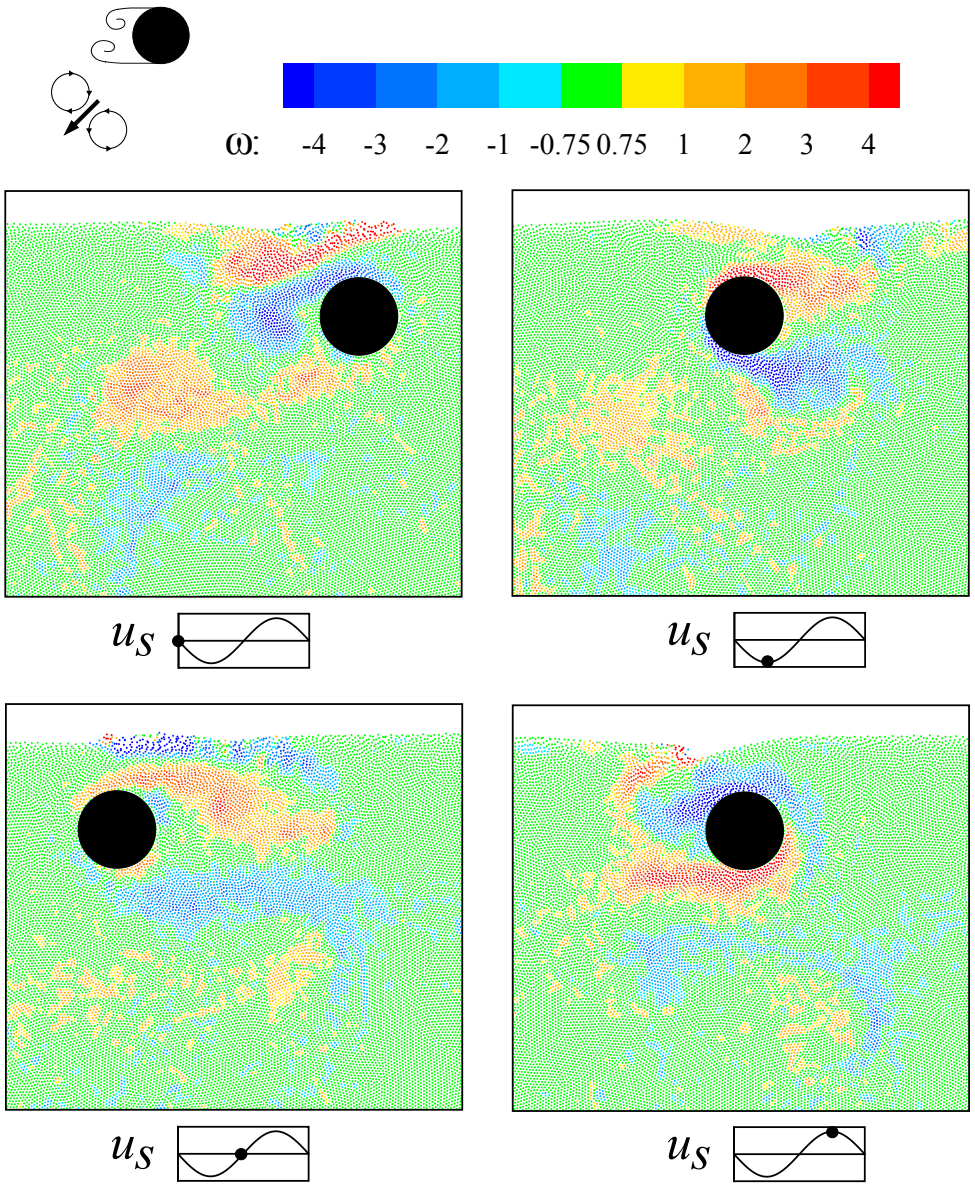

Figure : Vorticity contour at KC $= 10$ and $H/D = 0.75$.

Transverse vortex street

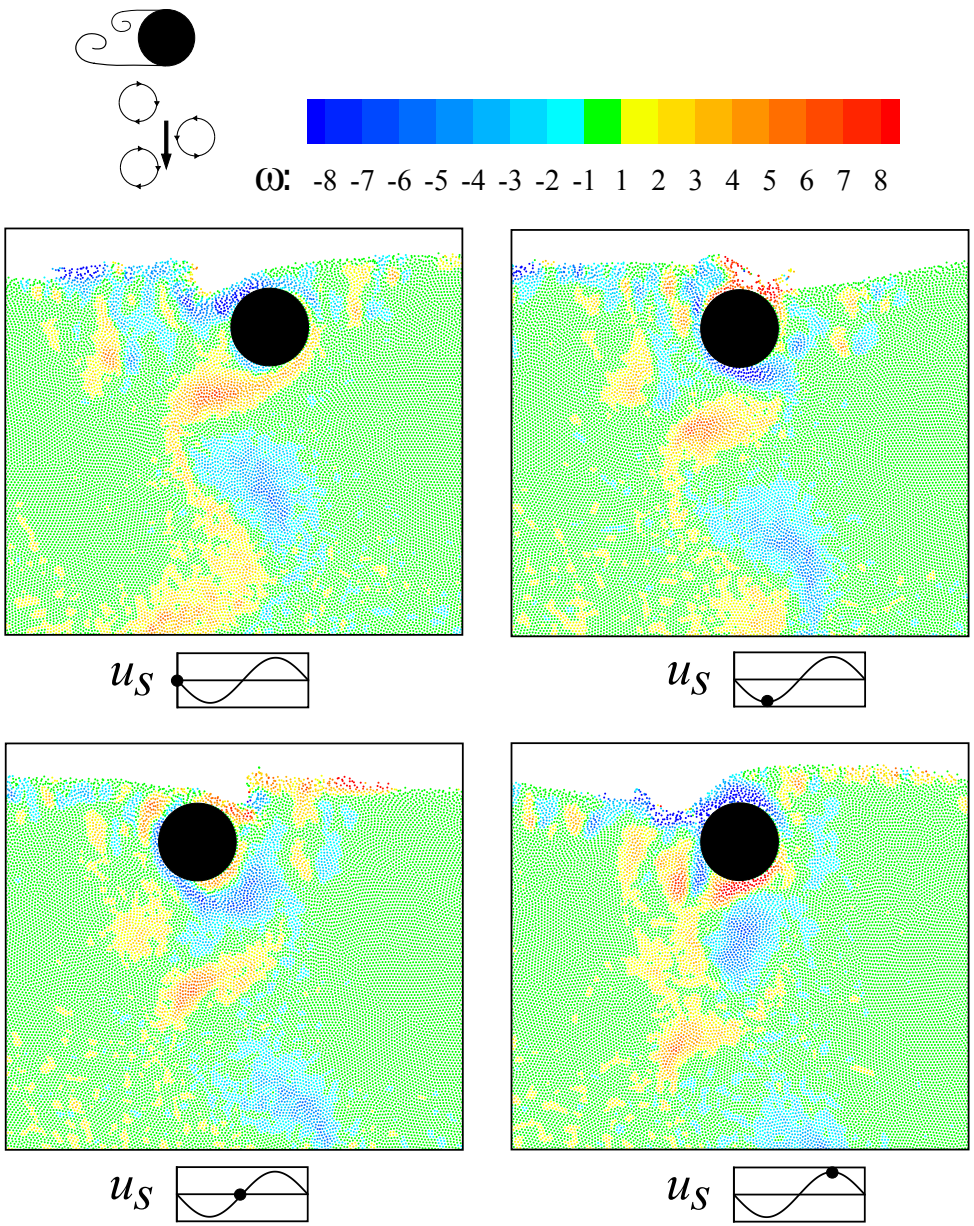

Figure : Vorticity contour at KC $= 3$ and $H/D = 0.5$.

Spectrum analysis of in-line force coefficient.

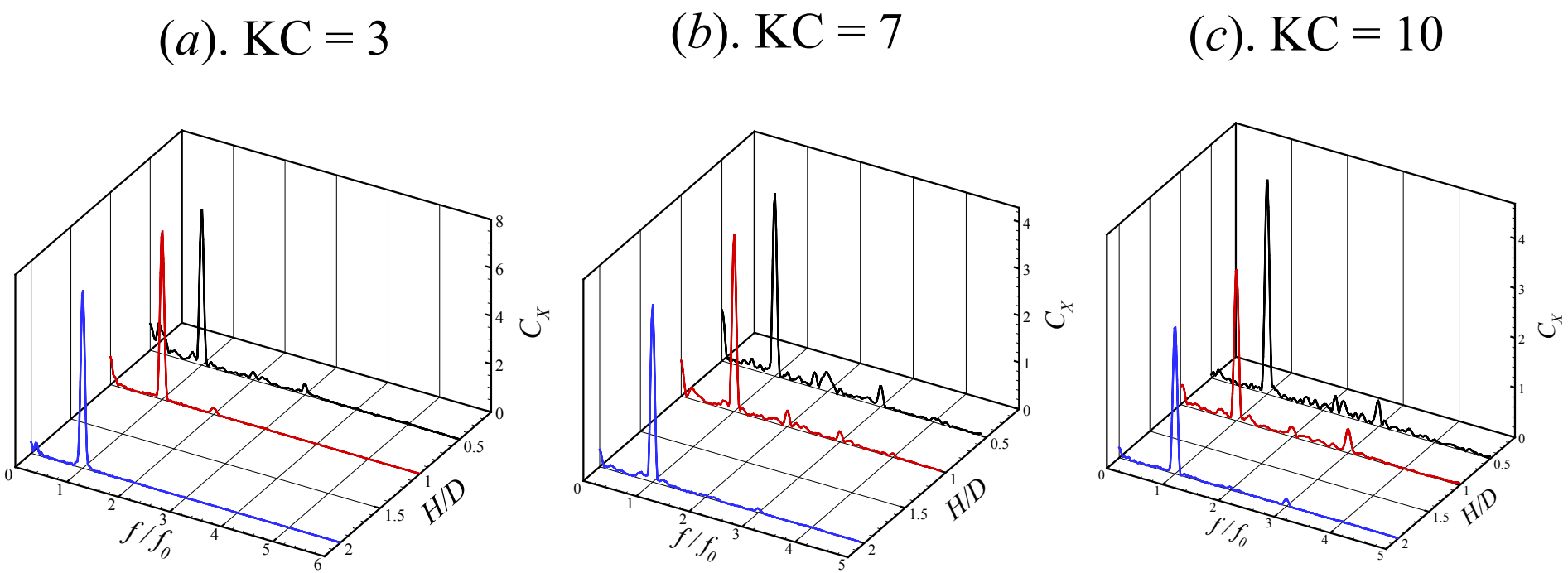

Figure : For all KC numbers and gap ratios, the fundamental frequency of the in-line force coefficient is the same as the frequency of cylinder oscillation.

Spectrum analysis of transverse force and free surface elevation at KC = 3

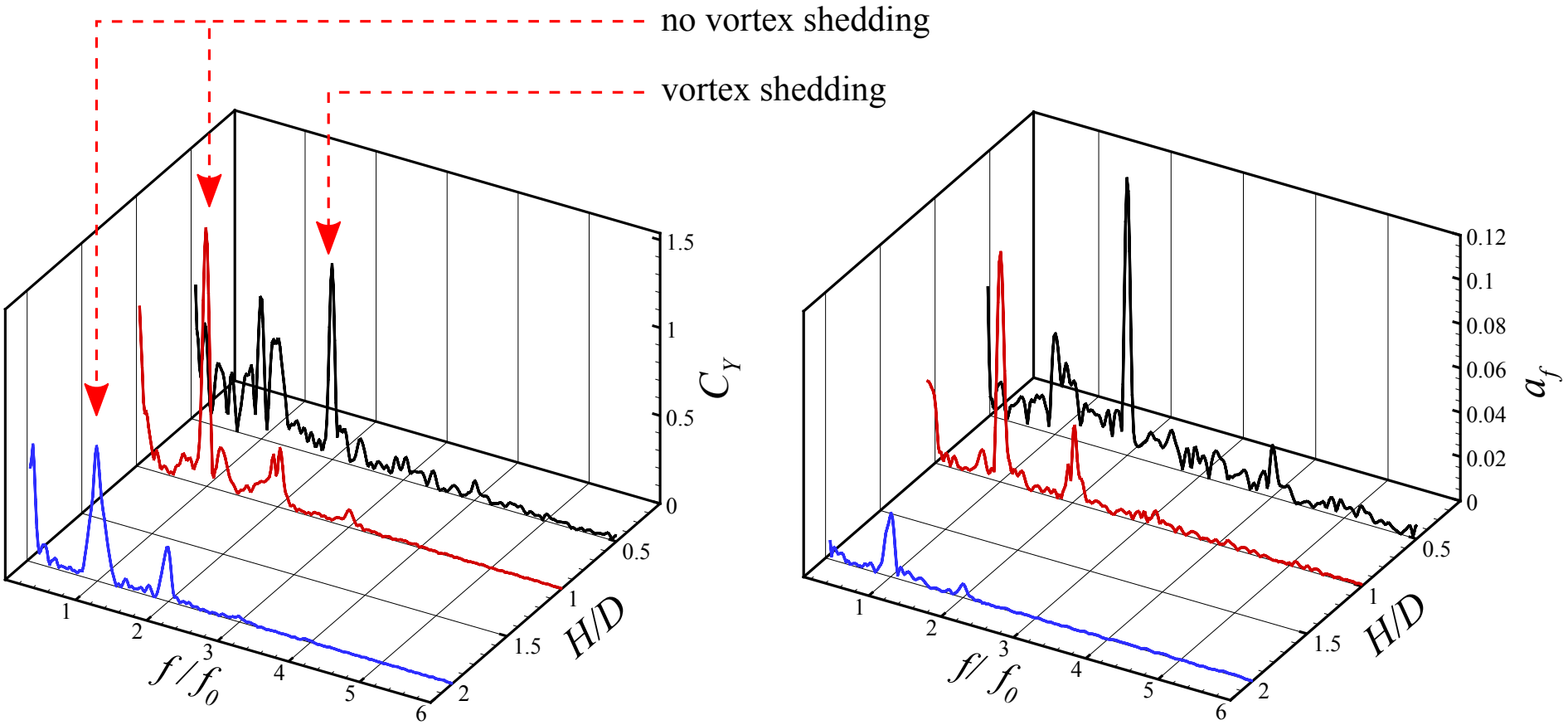

Figure : Right : transverse force coefficient; left : free surface elevation. The fundamental frequency of transverse force is the same as the fundamental frequency of free surface wave which suggests that the wave is generated by the transverse force.

Spectrum analysis of transverse force and free surface elevation at KC = 7 and 10

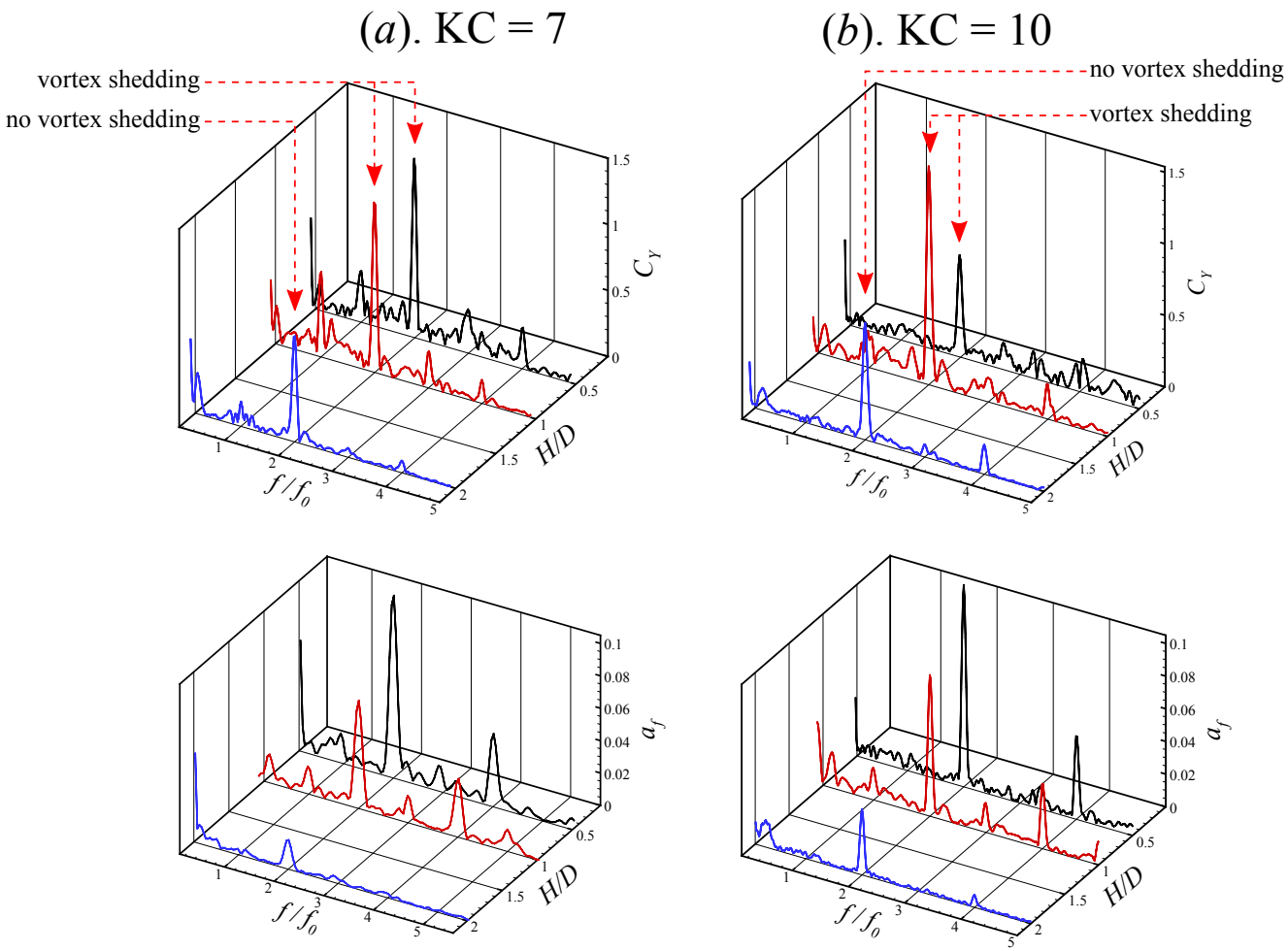

Figure : The fundamental frequency of the transverse force at KC = 7 and 10 are twice the frequency of cylinder oscillation for all gap ratios which is similar to the infinite fluid case. The fundamental frequencies of the free surface wave are also twice the frequency of cylinder oscillation.

Amplitude of free surface wave and transverse force coefficient as a function of H/D

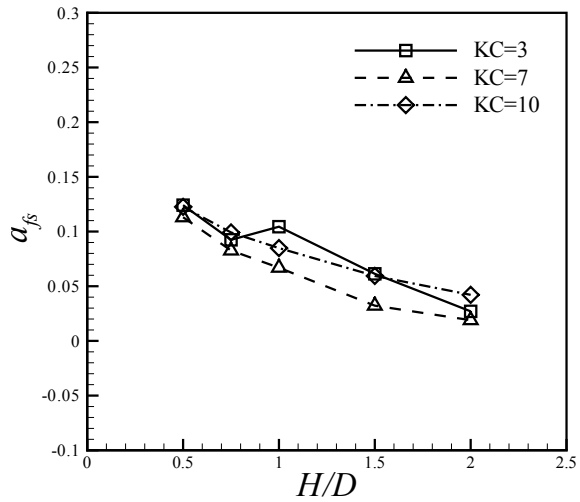

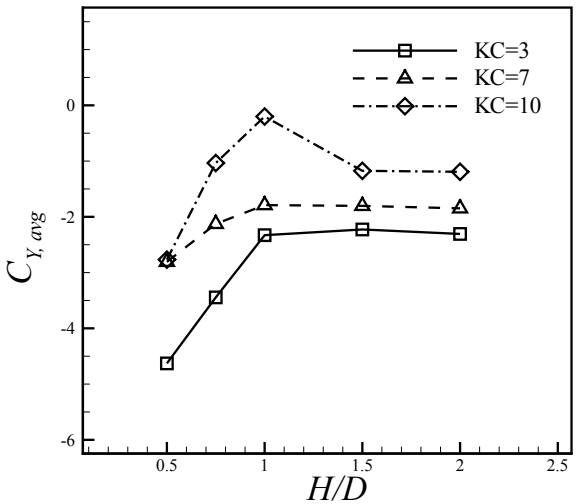

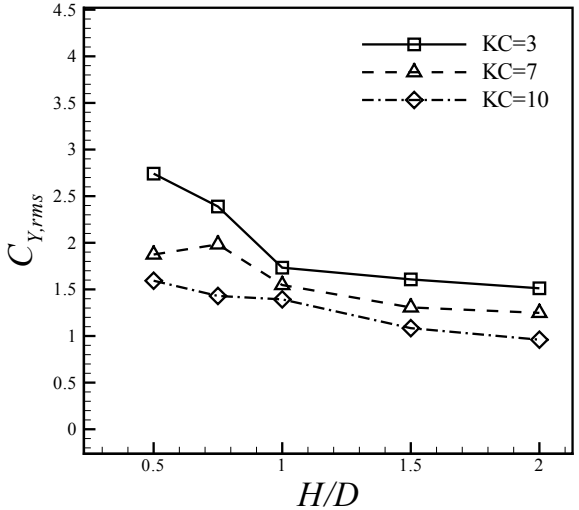

Figure : Top: The amplitude of free surface wave. Bottom left: the average transverse force coefficient. Bottom right: root mean square of the transverse force coefficient.

Conclusions

- We have developed a combined SPH-DFIB method based on the volume of solid function.
- The comparison of the results predicted by the present method with the benchmark results shows that the present method is able to achieve a comparable accuracy with a well established numerical method.
- The application of the present method to simulate the oscillating cylinder beneath a free surface reveals that
  1. the gap between the cylinder and the free surface affects the vortex formation and the transverse force,
  2. the free surface promotes vortex shedding, and
  3. the free surface wave is linked to the transverse force.

Thank you for your attention